NEU PRESS

ASREL Aerospace Research Letters

Cilt: 4 Sayı: 2 Yıl: 2025 | Araştırma Makalesi | e-ISSN: 2980-0064

Dynamic Analysis of the NREL/MIT Tension Leg Platform in OpenFAST

Muhammed UCAR[1] Nebi OZDONER[2*]

Necmettin Erbakan University, Engineering Faculty, Civil Engineering Department, Konya, Türkiye

Article Info

Received:
Accepted:
Published:

Keywords:
Floating Wind Turbines, Tension Leg Platform, Dynamic Analysis.

ABSTRACT

This study presents the dynamic analysis of the NREL/MIT tension leg platform (TLP) supporting the NREL 5-MW wind turbine using OpenFAST. The simulations represent environmental conditions specific to the Kıyıköy region in the western Black Sea. Selected Design Load Cases (DLCs) cover both response characterization and extreme sea states defined by IEC guidelines. The platform hydrodynamics are modeled using first-order potential-flow theory to capture primary motions and tendon tensions efficiently. Viscous and second-order effects are excluded to emphasize computational performance. Simulation durations are selected to allow consistent comparison. A computational cost assessment is also conducted. Results show that OpenFAST produces stable and realistic platform responses across all conditions while maintaining low computational demand. The study confirms the capability of time-efficient modeling for preliminary assessments of floating wind turbines in regional environments such as Kıyıköy.

NREL/MIT Gergi Ayaklı Platformunun OpenFAST'ta Dinamik Analizi

Makale Bilgisi

Geliş Tarihi:
Kabul Tarihi:
Yayın Tarihi:

Anahtar Kelimeler:
Denizüstü Rüzgar Tirbünleri, Gergi Ayaklı Platformlar, Dinamik Analiz.

ÖZET

Bu çalışma, NREL 5-MW rüzgar türbinini destekleyen NREL/MIT gergi ayaklı platformun (TLP) dinamik analizini OpenFAST kullanarak sunmaktadır. Simülasyonlar, Batı Karadeniz'deki Kıyıköy bölgesine özgü çevresel koşulları temsil etmektedir. Seçili Tasarım Yük Durumları (DLC'ler), IEC yönergeleri tarafından tanımlanan hem platform tepki karakteristiği tanımlayıcı hem de aşırı deniz durumlarını kapsamaktadır. Platform hidrodinamiği, birincil hareketleri ve tendon gerilimlerini verimli bir şekilde yakalamak için birinci dereceden potansiyel akış teorisi kullanılarak modellenmiştir. Hesaplama performansını vurgulamak için viskoz ve ikinci dereceden etkiler hariç tutulmuştur. Simülasyon süreleri tutarlı değerlendirmeye uygun seçilmiştir. Ayrıca bir hesaplama maliyeti değerlendirmesi de yürütülmüştür. Sonuçlar, OpenFAST'ın düşük hesaplama talebini korurken tüm koşullarda kararlı ve gerçekçi platform tepkileri ürettiğini göstermektedir. Çalışma, Kıyıköy gibi bölgesel ortamlarda yüzen rüzgar türbinlerinin ön değerlendirmeleri için zaman açısından verimli modelleme yeteneğini doğrulamaktadır.

Bu makaleye atıfta bulunmak için:

Ucar, M., & Ozdoner, N. (2025). Dynamic analysis of the NREL/MIT tension leg platform in OpenFAST. *Aerospace Research Letters (ASREL), 4*(2), 252-266.

***Sorumlu Yazar:** Nebi Ozdoner, *nozdoner@erbakan.edu.tr*

INTRODUCTION

Floating wind turbine (FWT) technology enables renewable energy harvesting in deep waters where fixed-bottom foundations are not feasible. Various platform types have been developed, including spar-buoy, semi-submersible, and tension leg platforms (TLPs), each offering distinct stability and cost characteristics. Among them, TLPs provide high stiffness and small motion amplitudes due to their pretensioned mooring lines, making them suitable for large turbines and challenging environments (Oguz et al., 2018; Hmedi et al., 2022).

Recent studies have highlighted the increasing potential of the Turkish coastal zones for floating wind deployment. Caceoglu et al. (2022) identified the Kıyıköy region in the western Black Sea as one of the most promising locations for offshore wind development. Motivated by this, Ucar et al. (2025a) conducted a design-oriented feasibility study of a site-specific TLP concept. Ucar et al. (2025b) extended this work by evaluating the fatigue life of different concepts under long-term environmental conditions. The doctoral research of Ucar (2025) provides an interlinked approach combining hydrodynamics, fatigue assessment, and capacity-factor estimation.

Accurate modeling of floating wind platforms requires balancing fidelity and computational cost. High-fidelity computational fluid dynamics (CFD) models are used in diverse fluid flow solutions (Kumcu & Ucar, 2017; 2019; 2020; Kaya, 2019). The CFD approach provides high-fidelity flow resolution but demands substantial computational resources (Ucar & Kumcu, 2018; Savci et al., 2023; Ismayilli & Buker, 2024). Conversely, coupled aero-hydro-servo-elastic tools such as FAST (Fatigue, Aerodynamics, Structures, and Turbulence) and its successor OpenFAST (NREL, 2025) offer computationally efficient simulations with multi-fidelity. These codes have been validated with experimental and numerical studies (Oguz et al., 2018; Ucar et al., 2022; 2025c) and widely applied for coupled dynamics and fatigue analyses of various floating wind turbine systems (Ucar et al., 2025b; 2025c; Putra et al., 2023). Parallel computational advances have further increased the feasibility of such multi-fidelity simulations on modern high-performance computing clusters (Putra et al., 2024; 2025). For regional-scale assessments, this balance between efficiency and fidelity is crucial to explore multiple environmental scenarios at reasonable computational expense.

Building on this context, the present study performs a dynamic analysis of the NREL/MIT TLP supporting the NREL 5-MW reference wind turbine (RWT) under environmental conditions representative of the Kıyıköy region. The objective is to characterize the platform motions, mooring loads, and associated computational effort across representative Design Load Cases (DLCs) using the coupled OpenFAST environment. The results provide an informative basis for early-stage feasibility evaluations of floating wind concepts in the Black Sea region.

MODEL DESCRIPTION

The FWT platform used in this study was originally developed by Tracy (2007) at Massachusetts Institute of Technology (MIT), and its spoke length was readjusted by Matha (2010) from NREL to prevent the platform from pitch mode resonance. Therefore, it is named after NREL/MIT TLP.

NREL/MIT TLP supports the National Renewable Energy Laboratory (NREL) 5-MW Reference Wind Turbine. The RWT model enables reproducible comparisons between diverse concepts, including floating (Ucar et al., 2022; 2025c) and onshore units (Buyukzeren et al., 2024). Its key parameters, including rotor diameter, rated power, hub height, and mass distribution, are summarized in Table 1. The aerodynamic and control properties follow the original baseline controller developed by NREL for variable-speed, pitch-to-feather operation.

Table 1
NREL's 5 MW baseline turbine properties (Jonkman et al., 2009)

Property	Specification
Rated power	5 MW
Rotor orientation & configuration	Upwind, three blades, 61.5 m length
Rotor diameter, hub diameter & hub height	126 m, 3 m, 90 m
Wind speed: Cut-in, Rated, Cut-out	3 m/s, 11.4 m/s, 25 m/s
Cut-in rotor speed, Rated rotor speed	6.9 rpm, 12.1 rpm
Rated tip-speed	80 m/s
Overhang, Shaft tilt, Precone	5 m, 5°, 2.5°
Rotor mass	110,000 kg
Nacelle mass	240,000 kg
Tower mass	347,460 kg
CM location	-0.2 m, 0.0 m, 64.0 m
Control system	Variable-speed generator torque & collective active pitch (PI)

NREL/MIT TLP is shown in Figure 1, and its features are given in Table 2. The platform consists of a central column connected to four outer columns through four pontoons, each connected to two mooring lines providing restoring stiffness. While the main restoring mechanism is mooring, a concrete ballasting of 12.6 m is used for the platform, having a draft of 47.89 m. Therefore, the platform center of mass (CM) is located 40.61 m below the still water line (SWL).

Table 2
NREL/MIT TLP properties

Properties	Value
Platform diameter	18 m
Platform draft	47.89 m
Water depth	200 m
Mooring system spreading angle	90°
Average mooring system tension per line	3,931 kN
Concrete (ballast) mass	8,216 tons
Concrete height (from the platform bottom)	12.6 m
Total displacement	12,187 tons
Number of mooring lines	8
Fairlead distance from the center	27 m
Unstretched mooring-line length	151.73 m
Line diameter	0.127 m
Line mass per unit length	116.03 kg/m
Line extensional stiffness	1,500 MN
Average steel density	7850 kg/m
Average concrete density	2562.5 kg/m
Steel wall thickness	0.015 m
Platform center of mass (CM)	-40.612 m
Full system center of mass	-32.7957 m
Center of buoyancy	-23.945 m

Figure 1
Schematic view of NREL/MIT TLP and the six degrees of freedom about its center of mass (CM)

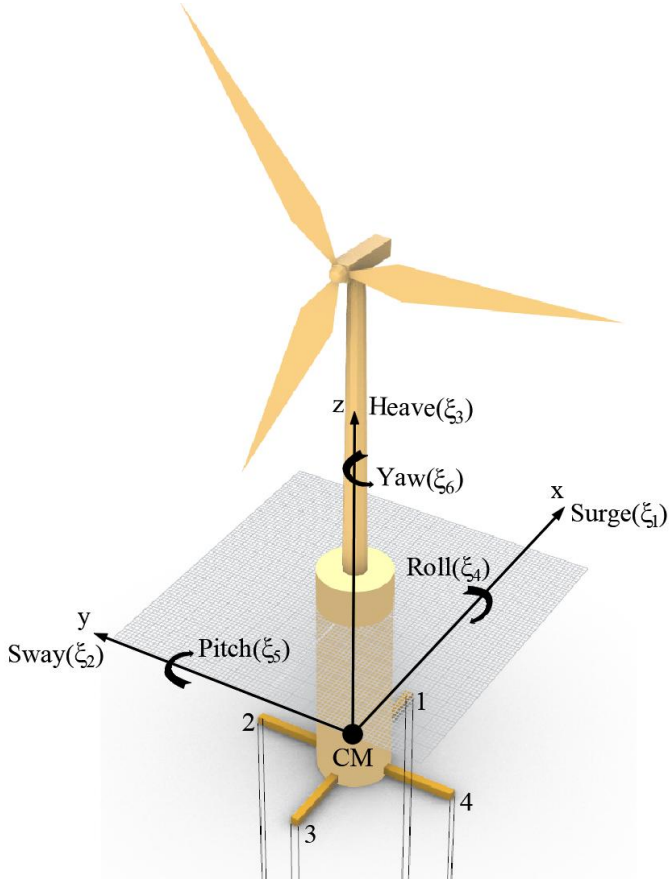

The simulations are performed using the coupled OpenFAST environment developed by NREL. This tool integrates aerodynamic, hydrodynamic, structural, and control modules into a time-domain solution framework:

- HydroDyn defines the first-order hydrodynamic loads based on potential-flow data and Morison elements.
- MoorDyn simulates the dynamic response of the mooring lines modeled as lumped-mass elements.
- AeroDyn calculates aerodynamic forces using blade element momentum theory (BEMT).
- ServoDyn governs pitch and generator control systems.

The overall modeling approach follows previous validation and fatigue studies conducted by the authors using OpenFAST and potential-flow solvers (Ucar, 2025; Ucar et al., 2025a; 2025b). For a potential flow solution, fluid is assumed ideal, i.e., inviscid and incompressible. The governing equation becomes time independent, and the outputs are frequency domain hydrodynamic coefficients and excitation forces. While being minor compared to diffraction effects, viscous effects are included with Morison-type hydrodynamic coefficients. The time-dependent problems with random wave patterns are solved using inverse Fourier transformations in HydroDyn to combine the frequency-domain outputs. The assumptions are common for preliminary studies for the sake of computational efficiency. On the other hand, for a detailed site-specific platform design, higher-order CFD solutions are required to consider turbulence and viscous effects despite high computational demand. The hydrodynamic behavior of the NREL/MIT TLP provides a baseline for comparing computational effort among different DLCs and identifying the demanding cases in terms of simulation time.

SIMULATION SETUP

All simulations were conducted using OpenFAST v3.6. Environmental inputs were defined according to the IEC 61400-3 guidelines (IEC, 2014). The 50-year extreme wind and wave condition values correspond to the long-term metocean analysis of the Kıyıköy site in the western Black Sea (Ucar, 2025). The sea-state parameters were previously derived from the joint probability distributions of significant wave height and peak period. The JONSWAP spectrum (Hasselmann et al., 1973) was used with a shape parameter $\gamma = 3.3$, and the wave direction was aligned or offset by 45° depending on the case definition.

The selected DLCs include static-equilibrium, free-decay, response characterization, and extreme conditions. Static-equilibrium and free-decay tests serve as initial validation. Static-equilibrium test is used to determine the initial orientation of the platform in the absence of external excitation. Then, the free-decay tests are conducted to calculate the platform's natural frequencies with its exponentially decaying motion. Response characterization cases are used to observe the wave-structure interactions under sinusoidal and non-sinusoidal waves. The extreme cases correspond to wind and wave events with a 50-year return period, determined by Ucar (2025) using extreme value analysis.

A summary of the simulated cases is given in Table 3. The simulations were executed on a workstation equipped with an Intel Core i5-12500H CPU and 16 GB RAM. The time step was selected to maintain numerical stability and ensure consistent coupling among the solver modules. For each DLC, the total CPU runtimes were recorded to assess computational performance.

Table 3
Design load cases (DLCs) and features

Load case	Description	Wind condition	Wave condition	Current condition
1.3a	Free decay-Surge	No air	Still water	-
1.3b	Free decay-Sway	No air	Still water	-
1.3c	Free decay-Heave	No air	Still water	-
1.3d	Free decay-Roll	No air	Still water	-
1.3e	Free decay-Pitch	No air	Still water	-
1.3f	Free decay-Yaw	No air	Still water	-
2.1	Regular waves	No air	Regular airy: Head waves, H=3 m, T=7 s	-
2.2a	Irregular waves	No air	Irregular airy: Head waves, H_s=3 m, T_p=7 s, JONSWAP spectrum	-
2.2b	Irregular waves	No air	Irregular airy: 45° waves. H_s=3 m, T_p=7 s, JONSWAP spectrum	-
2.5	50-year extreme wave	No air	Irregular airy: Head waves, H_s=7.25 m, T_p=15.75 s, JONSWAP spectrum	-
3.4	Wind/wave/current (WWC)	Steady, uniform, no shear: V_{hub}=8 m/s	Regular airy: Head waves, H=3 m, T=7 s	At surface, 0.5 m/s, reference depth=20 m
3.5	50-year extreme wind/wave	Turbulent (IECKaimal) V_{hub}=40 m/s	Irregular airy: Head waves, H_s=7.25 m, T_p=15.75 s, JONSWAP spectrum	-

RESULTS AND DISCUSSION

This section presents the numerical results obtained from the dynamic simulations of the NREL/MIT TLP under different environmental conditions. Once the platform's restoring characteristics are captured through the system identification, response characterization, and extreme load cases are conducted. Each simulation provides quantitative insight into the platform motions, tendon tensions, and computational effort required for each DLC. The results are discussed in relation to physical behavior and computational efficiency, emphasizing the balance between accuracy and runtime.

System Identification

System identification was performed through static-equilibrium and free-decay simulations to verify the physical consistency of the model. The static-equilibrium test yielded the platform's mean displacements and tendon tensions under steady conditions, while the free-decay analyses are used to identify the natural frequencies of the six rigid-body modes.

As presented in Table 4, the static-equilibrium results show that the NREL/MIT TLP remains well centered in all translational and rotational directions. The tendon forces are almost identical across all fairleads, with a mean value of approximately 3.9 MN, due to the symmetrically configured mooring system. The minor fore–aft difference in tendon pretension results from the 0.2-m rotor-nacelle assembly eccentricity shown in Table 1.

Table 4
Mean values for the static-equilibrium condition

	Surge (m)	Sway (m)	Heave (m)	Roll (°)	Pitch (°)	Yaw (°)	FL 1 (MN)	FL 2 (MN)	FL 3 (MN)	FL 4 (MN)
Value	-0.002	<0.001	0.007	<0.001	-0.003	<0.001	3.916	3.904	3.892	3.904

FL: Fairlead

The free-decay simulations produced the platform's natural frequencies, as listed in Table 5. The surge, sway, heave, and yaw modes agree well with the literature, with differences below 5% for surge, sway, and yaw and less than 0.1% for heave. These results verify that the platform's global stiffness and hydrodynamic coefficients are correctly represented. The pitch and roll frequencies are approximately 30% higher than the reference values, due to pitch–heave coupling and the associated restoring characteristics of the TLP.

Overall, the system identification results confirm that the model is stable, physically consistent, and suitable for time-domain simulations. The natural frequencies fall outside the first-order wave excitation range (0.04-0.25 Hz) according to DNV GL (2018), reducing the risk of resonance.

Table 5
Natural frequency comparison with reference values

Mode	Surge (Hz)	Sway (Hz)	Heave (Hz)	Roll (Hz)	Pitch (Hz)	Yaw (Hz)
Simulation	0.0158	0.0158	0.4367	0.2875	0.2883	0.0942
Reference	0.0165	0.0165	0.4375	0.2229	0.2211	0.0972
Difference	-4%	-4%	<0.1%	29%	30%	-3%

Response Characterization Cases

The response characterization cases include DLC 2.1, 2.2a, 2.2b, and 3.4. These simulations identify the platform's dynamic behavior under regular and irregular wave excitations and assess its coupled performance under steady wind and current.

Platform Motions

The platform motions for the response characterization cases are presented in Figure 2 and summarized in Table 6. Consistent with its high restoring stiffness, the TLP exhibits small amplitudes in constrained modes, heave, roll, pitch, and yaw. For the non-constrained modes, surge and sway, the mean motions are more parallel with the wind and wave excursion. Additionally, the decaying surge and sway mode motion up to around 300 s simulation time showed that the transitional duration may change with the modes. Sway, roll, and yaw mode motions under head waves are insignificant due to platform symmetry.

Under DLC 2.1 (Regular in Figures), surge mode motion reaches a maximum amplitude of 1.67 m and an RMS value of 0.56 m. For DLC 2.2a (Irregular in Figures), the maximum amplitude and the RMS are lower for the surge mode, while higher for the maximum amplitude in pitch mode. Pitch mode results are parallel with the maximum wave amplitudes, while it is valid for the RMS of the wave for the surge mode, due to the random phases and amplitudes of irregular waves.

For DLC 2.2b, where the wave direction is 45° (Irregular45° in Figures), surge and pitch amplitudes reduce, and sway and roll amplitudes increase, showing that oblique waves distribute excitation among degrees of freedom. Limited yaw motion (≈0.2°) develops under asymmetric wave loading, as expected.

The coupled DLC 3.4 case (WWC in Figures) includes steady wind and current in addition to regular waves, increasing the mean surge displacement due to aerodynamic thrust and current-induced hydrodynamic drag.

Mooring Line Tensions

The statistical results of the fairlead mooring tensions are summarized in Table 7. The mean tensions are close to 3.9 MN for all tendons, which is consistent with the pretension levels obtained in the static-equilibrium analysis. DLC 3.4 (WWC) is an exception due to the drag exerted by the wind and current. As shown in Figure 1, moorings 1-3 and 2-4 are opposite, and their responses are symmetric around the mean tension. Thus, only the fairlead mooring tensions of 1 and 2 are given in Figure 3. The minimum tensions occur at the downwind tendons (Mooring 1), and the upwind tendons experience the maximum simultaneously. No slack or breaking condition is observed.

Under DLC 2.1, the tendon tensions oscillate in parallel to the regular head waves, showing that the restoring stiffness of the tendons effectively balances the platform motions. In DLC 2.2a, irregular waves are introduced, and therefore, the random phasing of the wave components increases the dynamic range of tension. But it does not introduce significant asymmetry or excessive fluctuations.

For DLC 2.2b, the oblique wave direction changes the tension fluctuations. The two tendons facing the incoming waves experience higher peak loads due to the redistribution of wave-induced forces. Despite these variations, the RMS tension values remain close to those of the head-wave cases, confirming that the global stiffness and damping of the system prevent local overloads.

The coupled DLC 3.4 case introduces additional steady aerodynamic and current-induced forces; therefore, the mean tendon tensions show a small increase. The combination of steady and oscillatory loads does not lead to instability or nonlinear amplification.

Figure 2
Platform motions for response characterization cases

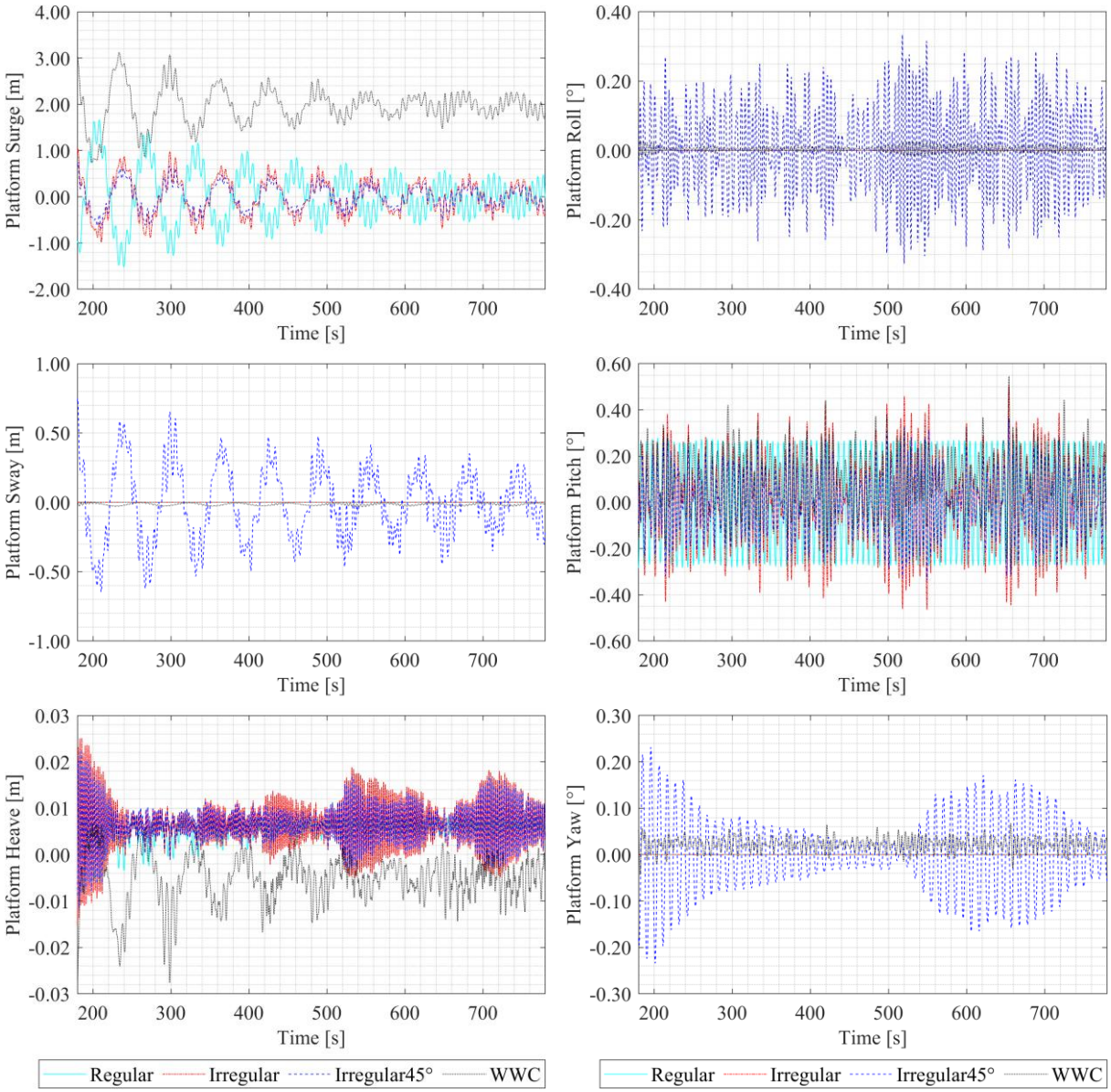

Figure 3
Fairlead mooring tensions for response characterization cases

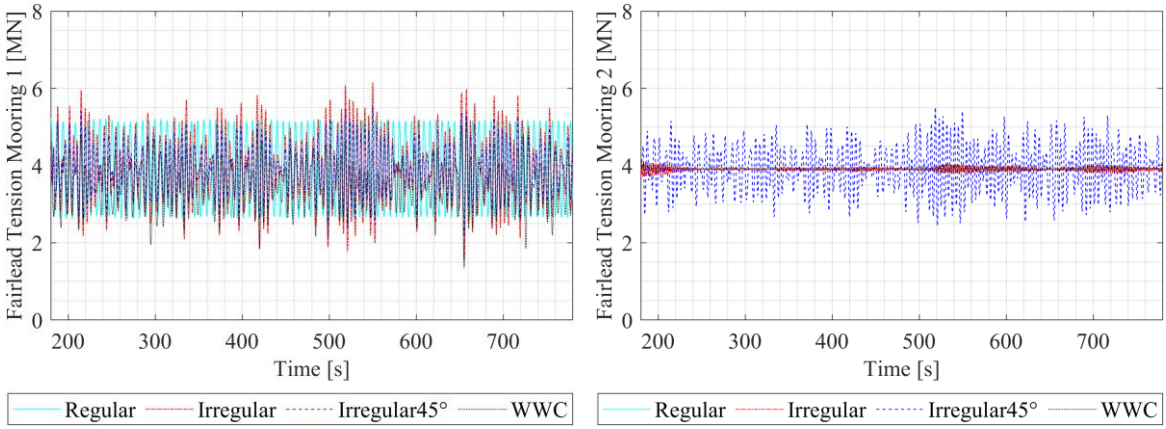

Extreme Cases

The extreme cases, DLC 2.5 and DLC 3.5, represent the most demanding environmental conditions simulated in this study. DLC 2.5 includes 50-year irregular head waves without wind, while DLC 3.5 combines 50-year extreme wind with irregular head waves.

Platform Motions

Figure 4 illustrates the platform motions in extreme cases, while the corresponding statistics are included in Table 6. Compared to the response characterization cases, the overall motion amplitudes increase significantly due to higher wave and wind excitation. In DLC 2.5 (Extreme Wave in Figures), the maximum surge amplitude reaches about 6 m, while the heave and pitch responses remain below 0.2 m and 0.6°, respectively. As in the response characterization cases, despite the energetic sea state, strong tendon restoring forces keep the constrained mode motions limited.

When wind loading is introduced in DLC 3.5 (Extreme Wind/Wave in Figures), the aerodynamic thrust shifts the maximum surge position forward to approximately 6.8 m. This is accompanied by the insignificantly higher heave maximum amplitude, below 0.2 m. The yaw response remains minor, confirming that the mooring layout effectively resists yawing motion. These results demonstrate that the TLP configuration can withstand combined aerodynamic and hydrodynamic loading without excessive displacement or instability.

The comparison between the two extreme cases shows that the addition of wind mainly affects surge maximum amplitude and mean offset, while its influence on heave and pitch remains limited within the typical operational envelope reported for similar TLP configurations (Oguz et al., 2018; Hmedi et al., 2022; Ucar et al., 2025c).

Mooring Line Tensions

Similar to the response characterization cases, the statistical results of the tendon tensions are summarized in Table 7, and only the Moorings 1 and 3 are given in Figure 5. Compared to wave response cases, higher maximum and lower minimum loads occur during the 50-year conditions due to the higher wave and wind excursions. Nevertheless, no slack or tendon breaking is observed. In both of the extreme cases, DLC 2.5 and 3.5, the minimum tension stays above 0.75 MN, which is 20% of the design pretension. The maximum tension stays below 7 MN, which is within the design range reported in previous numerical studies using the same platform (Matha, 2010).

In DLC 2.5, the maximum up-wave tendons experience peak tensions higher than the response characterization cases, and so the lower tensions for the down-wave tendons. On the other hand, the RMS and mean tensions remain close to the response characterization cases, due to facing similar oscillatory motions. On the other hand, in DLC 3.5, the extreme wind conditions exert high aerodynamic thrust, which increases the tendon loads in the upwind direction and decreases those for the downwind. Therefore, in DLC 3.5, the addition of extreme wind increases both mean and peak tensions. However, the slack or breaking mooring condition was not observed, showing that the mooring layout distributes forces effectively even under severe combined loading.

Overall, the mooring system supports structural integrity under both hydrodynamic and coupled extremes. The tension amplitudes are physically consistent with the corresponding surge displacements and do not indicate any tendency toward slack or resonance. These results confirm that the NREL/MIT TLP exhibits adequate stiffness, load distribution, and stability under 50-year extreme wind and wave conditions of the Kıyıköy region.

Figure 4
Platform motions for extreme cases

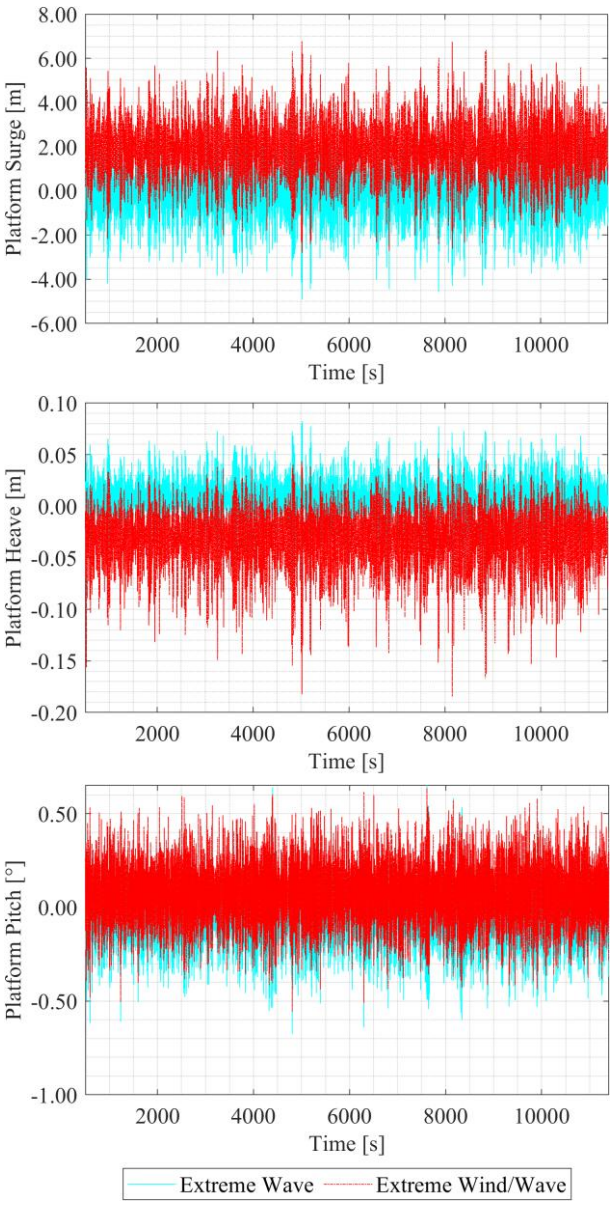

Figure 5
Fairlead mooring tensions for extreme cases

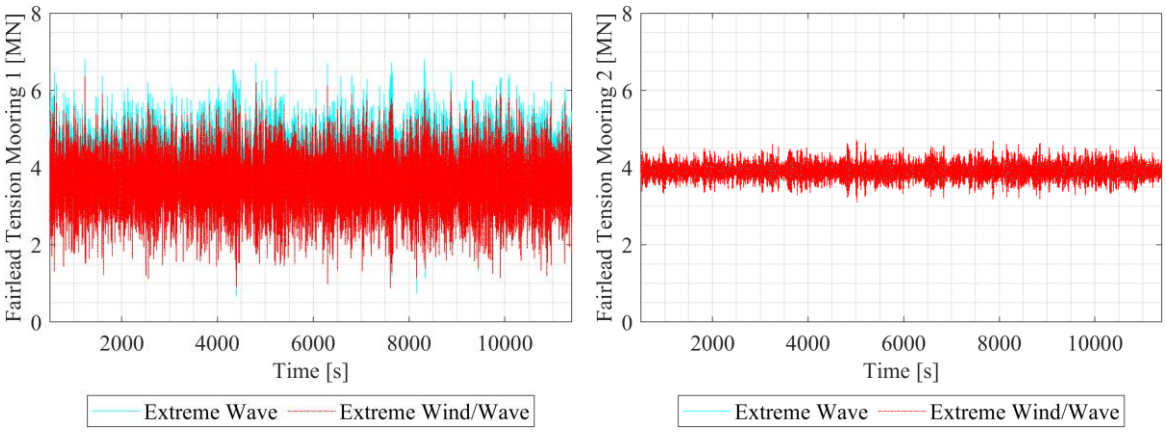

Table 6
Platform motions

Metric	DLC	Wave Elevation (m)	Surge (m)	Heave (m)	Pitch (°)	Yaw (°)
Maximum amplitudes	2.1	1.50	1.67	0.01	0.28	<0.01
	2.2a	2.52	1.04	0.03	0.50	<0.01
	2.2b	2.52	0.74	0.02	0.37	0.23
	2.5	7.90	6.14	0.14	0.68	<0.01
	3.4	2.52	3.13	0.03	0.55	0.07
	3.5	7.90	6.77	0.18	0.64	0.12
RMS	2.1	1.06	0.56	0.01	0.19	<0.01
	2.2a	0.65	0.37	0.01	0.18	<0.01
	2.2b	0.65	0.26	0.01	0.13	0.08
	2.5	1.84	1.37	0.02	0.17	<0.01
	3.4	0.65	1.99	0.01	0.15	0.03
	3.5	1.83	2.33	0.05	0.17	0.06
Mean	2.1	<0.01	0.01	0.01	<0.01	<0.01
	2.2a	<0.01	-0.01	0.01	<0.01	<0.01
	2.2b	<0.01	-0.01	0.01	<0.01	<0.01
	2.5	<0.01	<0.01	<0.01	<0.01	<0.01
	3.4	<0.01	1.95	-0.01	0.09	0.02
	3.5	<0.01	1.89	-0.04	0.07	0.06

Table 7
Fairlead mooring tensions

Metric	DLC	Wave Elevation (m)	Fairlead 1 (MN)	Fairlead 2 (MN)	Fairlead 3 (MN)	Fairlead 4 (MN)
Maximum amplitudes	2.1	1.50	5.23	3.92	5.21	3.92
	2.2a	2.52	6.15	4.09	6.25	4.09
	2.2b	2.52	5.52	5.51	5.60	5.48
	2.5	7.90	6.81	4.65	6.92	4.65
	3.4	2.52	5.26	4.05	6.45	4.01
	3.5	7.90	6.36	4.72	6.95	4.76
RMS	2.1	1.06	4.02	3.90	3.99	3.90
	2.2a	0.65	4.00	3.90	3.98	3.90
	2.2b	0.65	3.95	3.96	3.94	3.94
	2.5	1.84	4.00	3.91	3.98	3.91
	3.4	0.65	3.51	3.92	4.38	3.88
	3.5	1.83	3.67	3.91	4.33	3.96
Mean	2.1	<0.01	3.92	3.90	3.89	3.90
	2.2a	<0.01	3.92	3.90	3.89	3.90
	2.2b	<0.01	3.91	3.91	3.90	3.89
	2.5	<0.01	3.92	3.91	3.89	3.91
	3.4	<0.01	3.46	3.92	4.35	3.88
	3.5	<0.01	3.60	3.91	4.27	3.95

Computational Performance

The computational performance of the simulations is summarized in Table 8. The calm water cases, including static-equilibrium and the free-decay series (DLC 1.3a–1.3f), achieved high efficiency with simulation-to-elapsed-time ratios between 6.49 and 7.02. These values reflect the low computational cost when only structural and hydrodynamic solvers are active. For the regular and irregular wave cases (DLC 2.1, 2.2a, 2.2b), the ratios ranged from 3.26 to 4.80, indicating the additional cost of computing wave kinematics and hydrodynamic loads at each time step. The coupled case (DLC 3.4) showed a similar ratio of 3.70, demonstrating that steady aerodynamic thrust and current do not significantly increase runtime at this time-step level.

The extreme sea state (DLC 2.5) reduced the ratio to 2.69 due to the longer physical duration and full irregular-wave loading. The most demanding run, DLC 3.5, yielded a ratio of 0.07, driven by the finer 0.00125 s time step required for numerical stability under extreme turbulent wind and large waves. Overall, the results show predictable and consistent scaling of OpenFAST with respect to model complexity and time-step refinement, especially compared to CFD applications (Ucar, 2021).

Table 8
Computational performance

Condition	Simulation duration		Elapsed time (s)	Time step (s)	Simulation duration/ Elapsed time (-)
	Transient (s)	Used (s)			
Static-equilibrium	0	1,200	172	0.0125	6.98
DLC 1.3a	0	1,200	171	0.0125	7.02
DLC 1.3b	0	1,200	172	0.0125	6.98
DLC 1.3c	0	1,200	185	0.0125	6.49
DLC 1.3d	0	1,200	173	0.0125	6.94
DLC 1.3e	0	1,200	180	0.0125	6.67
DLC 1.3f	0	1,200	173	0.0125	6.94
DLC 2.1	180	600	125	0.0125	4.80
DLC 2.2a	180	600	184	0.0125	3.26
DLC 2.2b	180	600	125	0.0125	4.80
DLC 2.5	600	11,400	4,233	0.0125	2.69
DLC 3.4	180	600	162	0.0125	3.70
DLC 3.5	600	11,400	161,499	0.00125	0.07

CONCLUSIONS

This study analyzed the dynamic behavior of the NREL/MIT TLP supporting the NREL 5-MW wind turbine under Kıyıköy site conditions using OpenFAST. The simulations covered representative DLCs to assess platform motions, mooring tensions, and computational performance.

The results showed realistic responses in all conditions. Surge dominated the motion, while heave and pitch remained smaller than 0.2 m and 1° due to the tendons' high vertical stiffness. Directional waves reduced surge and pitch amplitudes and induced minor sway, roll, and yaw, consistent with expected behavior for oblique seas. The platform survived under 50-year extreme wind and wave conditions. Mooring loads stayed within the design limits; no breaking condition was observed, and the minimum tension was observed at 20% of the design pretension.

Overall, the study confirms that OpenFAST enables time-efficient simulations of TLP-type FWTs, providing a practical tool for early-stage decisions.

Ethical Statement

No Need.

Author Contributions

Research Design (CRediT 1) Author 1 (100%)

Data Collection (CRediT 2) Author 1 (100%)

Research - Data Analysis - Validation (CRediT 3-4-6-11) Author 1 (100%)

Manuscript Writing (CRediT 12-13) Author 1 (100%)

Revision and Improvement of the Text (CRediT 14) Author 1 (50%) - Author 2 (50%)

Funding

No.

Conflict of Interest

The authors declare that they have no known competing financial interests or personal relationships that could have appeared to influence the work reported in this paper.

Sustainable Development Goals (SDGs)

Sustainable Development Goals: 7 Affordable and Clean Energy.

REFERENCES

Buyukzeren, R., Kaya, M. N., Bacakoglu, A. A., Ucar, M., Altıntas, H. B., Ozturk, A., & Bilici, A. Y. (2024). Yatay Eksenli Rüzgâr Türbinlerinde Kule Yüksekliği ve Türbülans Yoğunluğu Etkisinin İncelenmesi. *Necmettin Erbakan Üniversitesi Fen ve Mühendislik Bilimleri Dergisi*. https://doi.org/10.47112/neufmbd.2024.66

Caceoglu, E., Yildiz, H. K., Oguz, E., Huvaj, N., & Guerrero, J. M. (2022). Offshore wind power plant site selection using Analytical Hierarchy Process for Northwest Turkey. *Ocean Engineering*, *252*, 111178. https://doi.org/10.1016/j.oceaneng.2022.111178

DNV GL. (2018). *DNVGL-ST-0119: Floating Wind Turbine Structures*. https://rules.dnv.com/docs/pdf/DNV/ST/2018-07/DNVGL-ST-0119.pdf

Hasselmann, K., Barnett, T. P., Bouws, E., Carlson, H., Cartwright, D. E., Enke, K., Ewing, J. A., Gienapp, A., Hasselmann, D. E., Kruseman, P., & others. (1973). Measurements of wind-wave growth and swell decay during the Joint North Sea Wave Project (JONSWAP). *Ergaenzungsheft Zur Deutschen Hydrographischen Zeitschrift, Reihe A*.

Hmedi, M., Uzunoglu, E., Medina-Manuel, A., Mas-Soler, J., Vittori, F., Pires, O., Azcona, J., Souto-Iglesias, A., & Guedes Soares, C. (2022). Experimental Analysis of CENTEC-TLP Self-Stable Platform with a 10 MW Turbine. *Journal of Marine Science and Engineering*, *10*(12), 1910. https://doi.org/10.3390/jmse10121910

IEC. (2014). IEC 61400-3-2:Design requirements for floating offshore wind turbines. *Wind Energy Generation System—Part*, 2–3.

Ismayilli, A., & Buker, M. S. (2024). İHA larda İtki İçin Kullanılan Mikro Turbojet Motorun Hava Kompresörünün Termodinamik Analizi. *ASREL*. https://doi.org/10.56753/ASREL.2024.3.3

Jonkman, J., Butterfield, S., Musial, W., & Scott, G. (2009). *Definition of a 5-MW reference wind turbine for offshore system development*.

Kaya, M. N. (2019). *Aerodynamic Design and Optimization of a Swept Horizontal Axis Wind Turbine Blade* [Doctoral dissertation]. Konya Technical University.

Kumcu, S. Y., & Ucar, M. (2017). *Dairesel kesitli dusulu bacalarda hava-su karısımının deneysel calısma ve CFD modelleme ile analizi*.

Kumcu, S. Y., & Ucar, M. (2019). Effect of Experimental and Mathematical Modeling of Spillway on Dam Safety. *Advances in Safety Management and Human Factors: Proceedings of the AHFE 2018 International Conference on Safety Management and Human Factors, July 21-25, 2018, Loews Sapphire Falls Resort at Universal Studios, Orlando, Florida, USA 9*, 296–305.

Kumcu, S. Y., & Ucar, M. (2020). KÖPRÜ BARAJI DOLUSAVAK YAPISININ DENEYSEL ÇALIŞMA VE SAYISAL MODELLEME İLE ANALİZİ. *Ömer Halisdemir Üniversitesi Mühendislik Bilimleri Dergisi*. https://doi.org/10.28948/ngumuh.515220

Matha, D. (2010). *Model development and loads analysis of an offshore wind turbine on a tension leg platform with a comparison to other floating turbine concepts: April 2009*.

NREL. (2025). *OpenFAST Documentation*. https://openfast.readthedocs.io/en/main/

Oguz, E., Clelland, D., Day, A. H., Incecik, A., López, J. A., Sánchez, G., & Almeria, G. G. (2018). Experimental and numerical analysis of a TLP floating offshore wind turbine. *Ocean Engineering*, *147*, 591–605. https://doi.org/10.1016/j.oceaneng.2017.10.052

Putra, M. J., Oğuz, E., & Uzol, N. S. (2025). Investigation of Energy Production of an Offshore Wind Farm Using FAST.Farm's Dynamic Wake Meandering Model and FLORIS. In *Innovations in Sustainable Maritime Technology—IMAM 2025* (pp. 420–432). Springer Nature Switzerland. https://doi.org/10.1007/978-3-032-01566-2_33

Putra, M. J., Sezer Uzol, N., Ucar, M., & Oguz, E. (2024). *Numerical Simulations of Floating Offshore Wind Turbines using Open-Source Codes on HPC*.

Savci, M., Hizalan, O., Metin, M., Karaduman, Y. E., Topcam, A. M., Ozgoren, M., & Demirsöz, M. (2023). Diverter in Hava Aliği Performansına Etkisinin Had Analizleriyle İncelenmesi. *ASREL*. https://doi.org/10.56753/ASREL.2023.2.2

Tracy, C. C. H. (2007). *Parametric design of floating wind turbines*. Massachusetts Institute of Technology.

Ucar, M. (2021). *Mathematical Modelling of Air-Water Flow Structure in Circular Dropshafts* [Master's thesis]. Necmettin Erbakan University.

Ucar, M. (2025). *Site-specific development and fatigue evaluation of a tension leg platform for floating wind deployment in Türkiye* [Doctoral dissertation]. METU.

Ucar, M., Hmedi, M., Uzunoglu, E., & Oğuz, E. (2025). Design and Analysis of a Floating Wind Turbine for the Kıyıköy Region, Türkiye. In *Innovations in Sustainable Maritime Technology—IMAM 2025* (pp. 433–445). Springer Nature Switzerland. https://doi.org/10.1007/978-3-032-01566-2_34

Ucar, M., Hmedi, M., Uzunoglu, E., & Oguz, E. (2025a). Effect of panel method codes in estimating the time-domain responses of floating wind turbines. *Brodogradnja: An International Journal of Naval Architecture and Ocean Engineering for Research and Development*, *76*(2), 1–31.

Ucar, M., Hmedi, M., Uzunoglu, E., & Oguz, E. (2025b). Fatigue load evaluation of multiple floating wind turbine systems. *Ocean Engineering*, *330*, 121101.

Ucar, M., & Kumcu, S. Y. (2018). Comparison of physical modeling and CFD simulation of flow over spillway in the Arkun Dam. *Proc. of 5th International Symp. on Dam Safety*.

Ucar, M., Uzunoglu, E., & Oguz, E. (2022). Comparison and Evaluation of Open-Source Panel Method Codes against Commercial Codes. *Gemi ve Deniz Teknolojisi*, *221*, 86–108. https://doi.org/10.54926/gdt.1106386